Eng. & Technology, Vol.24, No. 7, 2005

An Assessment of Transonic Flow on NACA Airfoil With K-Epsilon Standard, RNG and Spalart Turbulent Models Using A Quadrilateral Grid

Dr. Fayadh M. Abed Al-Dulaimy*
Received on: 21/9/2004
Accepted on: 6/10/2005

Abstract

The main objective of the present work is to investigate the characteristic of transonic viscous flow with standard k-ε , RNG and Spalart turbulent model using numerical technique matching and Fluent with quadrilateral type of grid generation in order to match with the boundary layer requirements. The computation is carried at Mach number 0.72. Two-dimensional 2822 airfoil at 2.8 angle of attack was studied. The numerical results show that the present model well predict the shock wave locations, strength and the change in flow properties due to geometry. The results show that the minimum nodal space (Y^+) for the k-epsilon model is 50 and for Spalart model is 30. Also the results were compared with the published data of the same geometry. It is concluded that the present results are in good agreement with the published data. The main emphasis is the comparison of numerical methods concerning the shock position and strength as well as the C_p, skin friction Distribution and point of separation.

Keyword: Computational fluid dynamics, Turbulence models, Transonic flow, spalart model, grid technique.

تقييم خصائص الجريان الصوتي لمقطع NACA مع استخدام موديل الجريان الاضطرابي سبالرت و K-Epsilon بنوعيه (Standard ,RNG) وبمساعدة النقاط الشبكية الرباعية.

الخلاصة

يهدف البحث الى دراسة خصائص الجريان الاضطرابي اللزج عند السرع الصوتية الحرجة ومن خلال استخدام ثلاث موديلات رياضية كل من (Standard K-Epsilon ,RNG) و سبالرت، حيث تم استخدام تقنيات التحليل العددي(Fluent) وبالموائمة مع استخدام تقنية تكوين النقاط الشبكية الرباعية للموائمة مع متطلبات سمك الطبقة المتاخمة. الحسابات أجريت عند سرعة جريان ماخ 0.72 ولمقطع 2822 وبيعدين وعند زاوية سقوط واحدة 2.8 درجة .تشير النتائج المتحققة الى ان اقل سمك لابعدي للنقاط الشبكية Y^+ هو 50 بالنسبة الى استخدام موديل k-epsilon و 30 مع استخدام موديل سبالرت. أظهرت النتائج المتحققة تطابق مع النتائج المنشوة. فقد اجريت مقارنة مع نتائج منشورة عمليا ونظريا فيما يخص موقع وشدة الموجات الصوتية وتوزيع معامل الضغط والاحتكاك ونقطة الانفصال.

Dept. of Control & Systems Engineering, UOT.

https://doi.org/10.30684/etj.24.7A.5
2412-0758/University of Technology-Iraq, Baghdad, Iraq

Nomenclatures

A= *Surface area vector*

A_f =*Area of face* $(|A_x i + A_z j|$

c_μ =Empirical coefficient

E =Empirical constant (9.81)

K =Von Karman's constant (0.42)

k =Turbulent kinetic nergy

K_p =Turbulent kinetic energy at point P

N_{face} =*Number of face enclosing cell*

S_ϕ = *Surface of* ϕ *per unit volume*

U_p =Mean velocity of the fluid at point P

v_f =*Mass flux though face*

V= *Cell Volume*

y_p =Distance from point P to the wall

ρ: *density*

v=*Velocity vector (ui+vj)*

Γ_ϕ =*Diffusion coefficient of* ϕ

$\nabla\phi$ =*Gradient of* $\left(\frac{\partial\phi}{\partial x}\right)i + \left(\frac{\partial\phi}{\partial y}\right)j$

$(\nabla\phi)_n$ = *Magnitude of* $\nabla\phi$ *normal to face*

φ_f =*Value of* ϕ *convected though face*

ε =Viscous dissipation rate

Introduction

It is an unfortunate fact that no single turbulence model is universally accepted as being superior for all classes of problems. The choice of turbulence model will depend on considerations such as the physics encompassed in the flow, the established practice for a specific class of problem, the level of accuracy required, the available computational resources, and the amount of time available for the simulation.

In turbulence models that employ the Boussinesq approach, the central issue is how the eddy viscosity is computed. The Boussinesq hypothesis is used in the Spalart-Allmaras model and the k-ε models. The advantage of this approach is the relatively low cost In the case of the Spalart-Allmaras model, only one additional transport equation (representing turbulent viscosity) is solved. In the case of the k-ε models, two additional transport equations (for the turbulent kinetic energy, k, and the turbulence dissipation rate, ε) are solved, and it is computed as a function of k and ε.

The model proposed by Spalart-Allmaras [1] solves a transport equation for a quantity that is a modified from the turbulent kinematics viscosity.

The Spalart and Allmaras model [2, 3] represents the last evolution of this class of models. This family does not follow the classical Prandtle's approach, where the model equation is obtained by the turbulent kinetics energy one. In particular in the Spalart and Allmaras model the equation is generated "from scratch" using empiricism and arguments of dimensional analysis [4].

The Spalart-Allmaras model was designed specially for aerospace applications involving wall-bounded flows and has been shown to give good results for boundary layers subjected to adverse pressure gradients. It is also gaining popularity for turbo machinery applications [5]. The Spalart-Allmaras model has been implemented to use wall functions

when the gradients of the transported variable in the model are much smaller than the gradients of the transported variables in the k-ε models [1]. This might make the model less sensitive to numerical error when non-layered meshes are used near walls.

The simplest "complete models" of turbulence are two-equation models in which the solution of two separate transport equations allow the turbulent velocity and length scales to be independently determined. The standard k-ε model falls within this class of turbulence model and has become the workhorse of practical engineering flow calculations in the time since it was proposed by Jones and Launder [6]. It is a semi-empirical model, and the derivation of the model equations relies on phenomenological considerations and empiricism.

As the strengths and weaknesses of the standard k-ε model have become known, improvements have been made to the model to improve its performance. Two of these variants are available in the present study, RNG k-ε model [7] and the standard k-ε model [8].

The purpose of the present study is the assessment of turbulent mode Spalart and the two versions of k-ε Standard and RNG models using Fluent code. In this paper the algorithm of the governing equations is well known, but the main points we emphasize are the way of using the present turbulent models, the efficiency, and verification of the validity in solving transonic flow.

The Standard k-ε Model Transport Equations for the Standard k-ε Model

The standard k-ε model is a semi-empirical model based on model transport equations for the turbulent kinetic energy (k) and its dissipation rate (ε). The standard k-ε model is therefore valid only for fully turbulent flows. In the standard $(k-\varepsilon)$ model, k and ε are obtained from the following semi-empirical transport equations [6]:

$$\rho\frac{\partial k}{\partial t} = \frac{\partial}{\partial x_i}\left[\left(\mu + \frac{\mu_t}{\sigma_k}\right)\frac{\partial k}{\partial x_i}\right] + \left.\begin{array}{l} \\ G + B - \rho\varepsilon - YM \end{array}\right\} \quad (1)$$

$$\rho\frac{\partial \varepsilon}{\partial t} = \frac{\partial}{\partial x_i}\left[\left(\mu + \frac{\mu_t}{\sigma_\varepsilon}\right)\frac{\partial \varepsilon}{\partial x_i}\right] + \left.\begin{array}{l} \\ C_1\frac{\varepsilon}{k}\left(G + C_3 B\right) - C_2\rho\frac{\varepsilon^2}{k} \end{array}\right\} \quad (2)$$

where C_1, C_2 and C_3 are empirical coefficients, and σ_k and σ_ε are the turbulent Prandtl/ Schmidt numbers for k and ε, respectively. The terms $C_1\left(\frac{\varepsilon}{k}\right)G$ and $C_2\rho\left(\frac{\varepsilon^2}{k}\right)$ in (2) represent, the shear generation and viscous dissipation processes of ε, respectively. G is a shear generation term $G = \mu_t S^2$ that represents the production of turbulent kinetic energy resulting from interactions between the mean flow and the turbulence fields. where S is the modulus of the mean rate-of-strain tensor, defined as

$S = \sqrt{2S_{ij}S_{ij}}$ and $S_{ij} = \frac{1}{2}\left(\frac{\partial u_i}{\partial x_j} + \frac{\partial u_j}{\partial x_i}\right)$ The term B is the buoyancy generation-destruction term $B = -\frac{\mu_t}{\rho\sigma_\rho}\rho g$ (depending on whether stratification is stable or unstable) that results from the fluctuating density field, where σ_ρ is the turbulent Prandtl/Schmidt number for density. The dilatation dissipation term, $YM = \rho\varepsilon^2\sqrt{\frac{k}{a^2}}$, is included in the k equation, this term is modeled according to a proposal by Sarkar [9]

Modeling the Effective Viscosity

The "eddy" or turbulent viscosity, μ_t is computed by combining k and ε as

$$\mu_t = c_\mu \rho \frac{k^2}{\varepsilon}$$

Model constants

The model constants have the following values [6]

Coef.	σ_k	σ_ε	C_1	C_2	C_μ
value	1.0	1.30	1.44	1.92	0.09

The RNG k-ε Model

Yakhot, *et al.* [7] have proposed another variant of the $(k-\varepsilon)$ model the performance characteristics of which are improved relative to the standard model. The proposed model is based on renormalized group theory [10], and is referred to as the "RNG" $(k-\varepsilon)$ model. The RNG $(k-\varepsilon)$ model employs an additional source/sink term in the ε equation. The values of the coefficients also differ from those of the Standard $(k-\varepsilon)$ model. The forms of the $(k-\varepsilon)$ equations of the RNG model are as follows

$$\rho\frac{\partial k}{\partial t} = \frac{\partial}{\partial x_i}\left(\alpha_k \mu_{eff}\frac{\partial k}{\partial x_i}\right) + \left.\begin{array}{l} \\ G + B - \rho\varepsilon - YM \end{array}\right\} \quad (3)$$

$$\rho\frac{\partial \varepsilon}{\partial t} = \frac{\partial}{\partial x_i}\left(\alpha_\varepsilon \mu_{eff}\frac{\partial \varepsilon}{\partial x_i}\right) + \left.\begin{array}{l} \\ c_{1}\frac{\varepsilon}{k}\left(G + C_3 B\right) - c_2^* \times \rho\frac{\varepsilon^2}{k} \end{array}\right\} \quad (4)$$

Where

$$c_2^* = \left\{ C_2 + \frac{C_\mu \rho \eta^3 \left(1 - \eta/\eta_0\right)}{1 + \beta\eta^3} \right\}$$

The extra term in (4) employs the parameter η, which represents the ratio of characteristic time scales of turbulence and the mean flow fields, defined by

$$\eta = s\frac{K}{\varepsilon} \text{ Where}$$

$$s = \sqrt{2s_{ij}s_{ij}} = \sqrt{G/\mu_t}$$

It can be shown that η is a function of the ratio of generation to dissipation of k and can be written as $\eta = \sqrt{c_\mu^{-1}\frac{G}{\rho\varepsilon}}$ which indicates that η characterizes the equilibrium

characteristics of the turbulence field.

The primary coefficients of the RNG model for isothermal flows are $C_\mu, C_1, C_2, \sigma_K$, and σ_ε. The other two coefficients, η_0 and β, can be obtained directly from the primary model coefficients and the VonKarman constant, k.

These values result in values of 4.38 and 0.012 for η_0 and $\beta_{,,}$ respectively, and are referred to as the "original" set of coefficients. The quantities α_k, and α_ε are the inverse effective Prandtl numbers for k and ε, equals 1.393 respectively. Yakhot *et al.*[7] recommend the following values for the primary set of model coefficients.

Coef.	σ_k	σ_ε	C_1	C_2	k
value	0.7	0.7	1.42	1.7	0.4

The above models have similar forms, with transport equations for k and ε .The major differences in the models are as follows:

- the method of calculating turbulent viscosity
- the turbulent Prandtl numbers governing the turbulent diffusion

of k and ε the generation and destruction terms in the (ε) equation.

Standard Wall Functions

The standard wall functions are based on the proposal of Launder and Spalding [11],

$$U^* = \frac{\rho U_p C_\mu^{1/4} K_p^{1/2}}{\tau_w}, \quad y^* = \frac{\rho C_\mu^{1/4} K_p^{1/2} y}{\mu}$$

The law-of-the-wall for mean velocity yields is valid for $y^* > 11.225$, When the mesh is such that $y^* < 11.225$ at the wall-adjacent cells, the laminar stress-strain relationship that can be used [12].

Spalart-Allmaras Model

The Spalart and Allmaras model belongs to the family of eddy viscosity models. This family of models is based on the assumption that Reynolds stress tensor $-\rho\overline{uv}$ is related to the mean strain rate through an apparent turbulent viscosity called eddy viscosity (ν_t) in the Spalart and Allmaras model, the eddy viscosity is computed through a partial differential equation

$$-\overline{uv} = \nu_t\left(\frac{\partial \bar{u}}{\partial y} + \frac{\partial \bar{v}}{\partial x}\right)$$

In particular the eddy viscosity is computed by an intermediate variable $\tilde{\nu}$ through the relation

$$\nu_t = \bar{\nu} f_{v1}(x)$$

Where χ is the ratio $\frac{\bar{\nu}}{\nu}$, and f_{v1} is a damping function. The intermediate variable is computed by solving a differential equation that can be written as

$$\rho\frac{D\bar{\nu}}{Dt} = G_\nu + \frac{1}{\sigma\nu}\left[\frac{\partial}{\partial x_j}\left\{\left(\mu + \rho\bar{\nu}\right)\frac{\partial \bar{\nu}}{\partial x_j}\right\} + C_{b2}\rho\left(\frac{\partial \bar{\nu}}{\partial x_j}\right)^2\right] - Y_\nu \quad (5.)$$

The transported variables in the Spalart-Allmaras model, $\bar{\nu}$, is

identical to the turbulent kinematics viscosity except in the near-wall (viscous affected) region [13].
In equation (5) G_v is the production of turbulent viscosity and Y_v is the destruction of turbulent viscosity that occurs in the near-wall region due to wall blocking and viscous damping, in particular $\sigma_{\tilde{v}}$ and C_{b2} denotes the turbulent Prandtl number and a calibration constant and v is the molecular kinematics viscosity

Modeling the Turbulent Viscosity

The turbulent viscosity, μ_t, is computed from

$$\mu_t = \rho \tilde{v} f v_1 \qquad (6.)$$

Where the viscous damping function, fv_1, is given by

$$fv_1 = \frac{x^3}{x^3 + C_{v1}^3} \qquad (7.)$$

And

$$x \equiv \frac{\tilde{v}}{v} \qquad (8.)$$

Flow physics

The Mach number of the free-stream flow is 0.72. The Reynolds number based on chord length of the airfoil and free-stream flow conditions is 6.2x10^6. Hence the flow is turbulent and compressible. Viscosity 1.983 x10^5 Pa-s, Conductivity, 0.0242 W/m-K, Specific heat, 1006.43 J/kg-K, static pressure is set to 43765 Pa, static temperature is 299.5 K and the angle of attack is equal to 2.8 degrees. Turbulent kinetic energy at the pressure-far-field is 0.125 m^2/s^2 and the turbulent dissipation rate is equal to 7.32 m^2/s^3. These values are taken from reference [14]. The static pressure was computed based on the specified Reynolds number and Mach number and an assumed value of static temperature. The computational flow field is initialized with uniform flow corresponding to these free stream conditions.

Computational Domain and Boundary Conditions

The computational domain for this case is bounded by a non-slip airfoil surface and a far field boundary placed a significant distance from the airfoil as shown in Fig. 1. In an external flow such as that over an airfoil, we have to define a far field boundary and mesh the region between the airfoil geometry and the far field boundary. It is a good idea to place the far field boundary well away from the airfoil since we'll use the ambient conditions to define the boundary conditions at the far field. The domain for the analysis is chosen such that the presence of the airfoil is not felt at the outer boundary of the domain. The far field boundary is the line ABCDEFA in Fig.1.

Mesh Generation

Successful computations of turbulent flows require some consideration during the mesh generation. Since turbulence (through the spatially-varying effective viscosity) plays a dominant role in the transport of mean momentum and other scalars for the majority of complex turbulent flows, you must ascertain that turbulence quantities are properly resolved, if high accuracy is required. Due to the strong interaction of the mean flow and turbulence, the numerical results for turbulent flows tend to be more susceptible to grid

dependency than those for laminar flows.

It is therefore recommended that we should resolve, with sufficiently fine meshes, the regions where the mean flow changes rapidly and there are shear layers with a large mean rate of strain.

This case has been numerically tested under the flow conditions that generate a transonic, turbulent, and a shock-induced separated flow environment. The structured grid for this case has been generated using the grid generator GAMBIT. In order to apply the production version of the grid generator and the flow solver suitable for two-dimensional flow. The grid has been generated with the objective of performing a wall function-based turbulent flow analysis. The nodal spacing of the immediate nodes off the surface has been specified to yield average Y+ = 50 (for a Reynolds number = 6.2x10^6). Should cluster grid points in region of high gradients, since the numerical error tends to increase in high gradient regions and we can compensate for this by decreasing Δx, and Δy. In high gradients regions clustering tends to decrease numerical error. Also the variation in grid spacing must be gradual, non gradual stretches increase numerical error and degrade convergence, generally for all adjacent grid cells we must follow $0.8 \leq \frac{\Delta_{i+1}}{\Delta_i} \leq 1.2$ [15]

Results and discussion

The flow field analysis in the present paper has been tested numerically corresponding to the free stream flow at a Mach number of 0.72, angle-of-attack of 2.8° and a Reynolds number of 6.2 million based on the unit chord of the airfoil. The flow computations required 1200 iterations to converge. At the end of this run, flow residue has been reduced by more than three orders of magnitude. Convergence of the computations via the history of the governing equations residue are shown in Figures 3, 4, and 5 respectively.

This case has been numerically tested under the flow conditions that generate a transonic, turbulent, and a shock-induced separated flow environment. The structured grid for this case has been generated using the grid generator GAMBIT.

The results are presented in a contour of Mach number shown in Figures.6, 7, and 8 respectively. These results showed that the shock wave is clearly visible on the upper surface of the airfoil. Plot of velocity profile along the upper surface of the airfoil at different position gives a good view to the boundary layer thickness as shown in Figures 9, 10 and 11. The results of pressure distribution as shown in Figures.12, 13 and 14 give a good indication to the position and strength of the shock wave in the different turbulent models in the same condition.

For this case, a shock is present on the upper surface of the airfoil which leads to a region of separated flow immediately aft of the shock. A comparison of the pressure distribution of the Spalart and k-epsilon (RNG) models results with published data are shown in Figure 15 and 16. The wake region behind trailing edge of 2822 airfoil can be visualized by plotting and zooming

the velocity vector as shown in figure 17.

An examination of the skin friction coefficients in figure 18, 19 and 20 indicates that the flow separates immediately downstream of the shock. The flow computed with the Spalart-Allmaras, model models re-attaches downstream of the shock before separating at the trailing edge. A comparison of Numerical predictions of the skin friction coefficient (Cf) with the Published data is shown in Figures 21. The agreement between the current predictions and the data is good. Also plot the skin friction coefficient of wall shear stress on the airfoil surface indicate a large pressure gradient induced by the shock causes the boundary layer to separate the point of separation is where the wall shear stress vanishes.

The results for the shock location and aerodynamic coefficients are compared with the published data are shown on table.1

The shock wave is clearly visible on the upper surface of the airfoil, where the pressure first jumps to a higher value The difference in the shock location of two version of k-epsilon models is due to fact that in RNG model the region where (η is less than $\eta 0$) the extra term makes a positive contribution, and the second term of extra function becomes larger than the first. In the logarithmic layer, for instance, it can be shown that η is greater than 3.0, giving second item greater than 2.0, which is close in magnitude to the value of first ittem of C2 of equati on 4. in the standard k-epsilon model. As a result, for weakly to moderately strained flows, the RNG model tends to give results largely comparable to the standard k-epsilon model, Thus, the RNG model is more responsive to the effects of rapid strain and streamlines curvature than the standard k-e model, which explains the superior performance of the RNG model for certain classes of flows, and this estimation can be approved through comparison with the published date as shown in Figures 23 and 24.

To assess the performance of the Turbulence models k-epsilon (standard and RNG version) and Spalart model with the transonic flow a 2822 airfoil is selected for computations, and an experimental data are available in literature. The grid has been generated with the objective of performing a wall function-based turbulent flow analysis. The nodal spacing of the immediate nodes off the surface has been specified to yield an average Y+ = 50 where $y^+ = \frac{y}{\mu}\sqrt{\rho\tau_w}$ (for a Reynolds number = 6.2x10^6) as shown in Fig.25. It is concluded that the shock location obtained using both the Spalart-Allmaras, and the K-epsilon (Standard and RNG) turbulence models agrees well with the published data.

Computational Effort: CPU Time and Solution Behavior

In terms of computation, the Spalart-Allmaras model is the least expensive turbulence models, since only one turbulence transport equation is solved.

The standard k-e model clearly requires more computational effort than the Spalart-Allmaras model since an additional transport equation is solved. However, due to the extra

terms and functions in the governing equations and a greater degree of nonlinearity, computations with the RNG k-e model tend to take 10-15% more CPU time than with the standard k-e model as shown in table 1.

Performance Characteristics

For simple flows in which turbulence is in local equilibrium, the RNG $k-\varepsilon$ model produces results similar to those of the standard $k-\varepsilon$ model. For off-equilibrium flows, however (especially those involving recirculation, where $G > \rho\varepsilon$, RNG model with the recommended set of revised coefficients often produces predictions that are less diffusive than those of the standard model, in the current study the results of both models are similar there is no recirculation

References

1. Spalart, P., and S. Allmaras. A one-equation turbulence model for aerodynamic flows. Technical Report AIAA-92-0439, American Institute of Aeronautics and Astronautics, 1992.
2. Spalart, P., and S. R. Allmaras. A One-equation Turbulence model for aerodynamic flows. AIAA Paper 92-0439.
3. Spalart, P., and S. R. Allmaras. A One-equation Turbulence model for aerodynamic flows. La recherche Aerospatial (1):5-21,1994.
4. Papadakis Lall , Papadakis Lall M., V., and K. A. Hoffman. Performance of turbulence models for planer flows: a selected review. AIAA Paper 94-1873.
5. Launder, B. E. and D. B. Spalding. The Numerical Computation of Turbulent Flows. *Computer Methods in Applied Mechanics and Engineering*, 3:269-289, 1974.
6. Launder, B. E. and D. B. Spalding. Lectures in Mathematical Models of Turbulence. Academic Press, London, England, 1972.
7. Yakhot, V. and S. A. Orszag. Renormalization Group Analysis of Turbulence: I. Basic Theory. Journal of Scientific Computing,1(1):1{51, 1986.
8. Shih, W. W. Liou, T.-H., A. Shabbir, and J. Zhu. A New k-_ Eddy- Viscosity Model for High Reynolds Number Turbulent Flows -Model Development and Validation. Computers Fluids, 24(3):227{238, 1995.
9. Sarkar, S. and L. Balakrishnan. Application of a Reynolds stress Turbulence Model to the Compressible Shear Layer. ICASE Report 90-18, NASA CR 182002, 1990.
10. Choudhury,D. Introduction to the Renormalization Group Method and Turbulence Modeling. Fluent Inc. Technical memorandum TM-107, 1993.
11. Launder, B. E. and D. B. Spalding. The Numerical Computation of Turbulent Flows. Computer Methods in Applied Mechanics and Engineering, 3:269{289, 1974.
12. Fayadh, M. Abed Al-Dulaimy,"Numerical Prediction of Transonic Viscous Flow with Turbulent Model Using Hybrid Grid Technique", Eng. & Technology, Vol.23, No.8, 2004

13. Chen, H. C. and V. C. Patel. Near-Wall Turbulence Models for Complex Flows Including Separation. AIAA Journal, 26(6):641{648, 1988.

14. Cook ,P.H. M.A. McDonald, M.C.P. Firmin, "Aerofoil RAE 2822 - Pressure Distributions, and Boundary Layer and Wake Measurements," *Experimental Data Base for Computer Program Assessment*, AGARD Report AR 138, 1979.

15. Thomas, H. and Lars, D., "Reynolds stress transport modeling of transonic flow around the RAE2822 airfoil," AIAA 94-0309, 1994.

16. Daryl Lawrence Bonhaus "An Upwind Multigrid Method for Solving Viscous Flows on Unstructured Triangular Meshes" B.S. June 1990, University of Cincinnati.

Table-1-

MODEL	*CL*	*CD*	*Sh-P*	*CPU time*
Spalart	*0.73*	*-0.02*	*0.51*	*20 min*
k-ε RNG	*0.8*	*-0.01*	*0.53*	*35 min*
K-ε Standard	*0.8*	*-0.02*	*0.52*	*30 min*

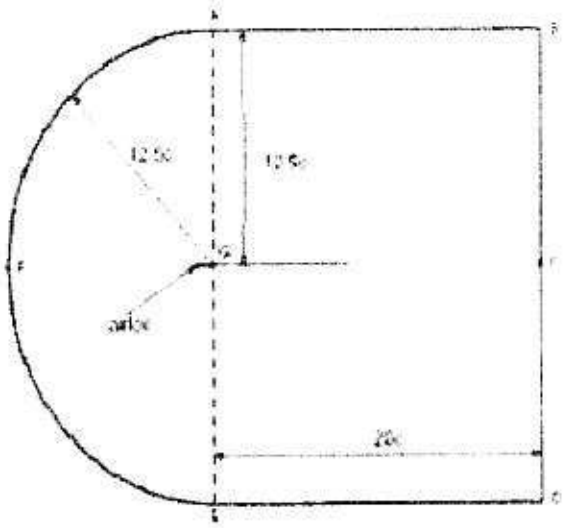

Fig.1 Computational domain and bboundary condition

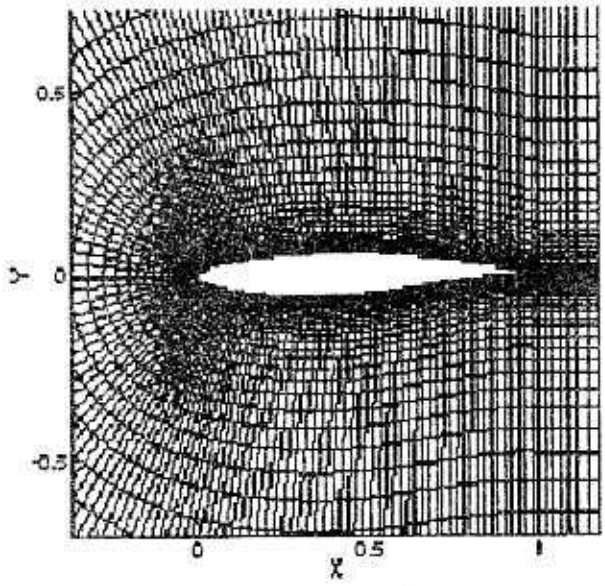

Fig.2 Mesh generation (C-type)

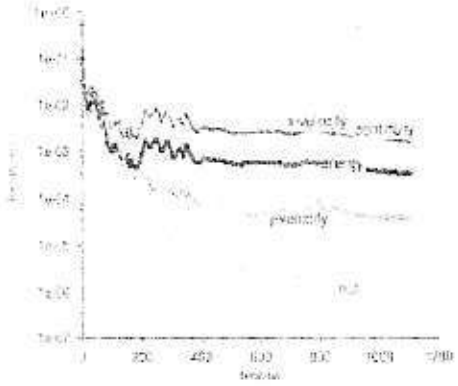

Fig 3 Convergence (Spalart model)

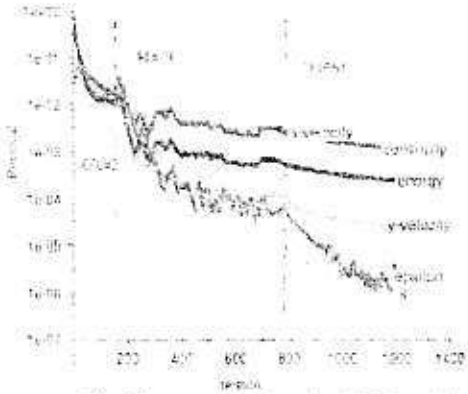

Fig 5 Convergence k-epsilon RNG model

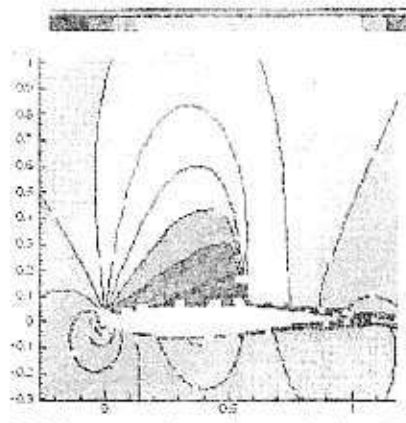

Fig 7 Mach contours (k-epsilon standard model)

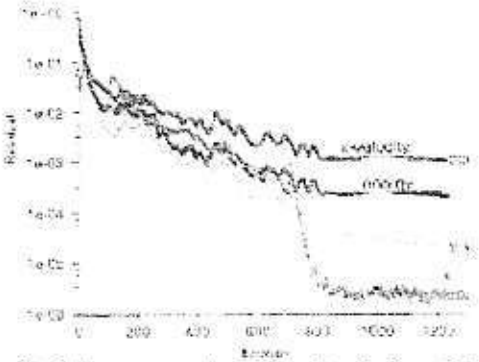

Fig 4 Convergence k-epsilon (standard model)

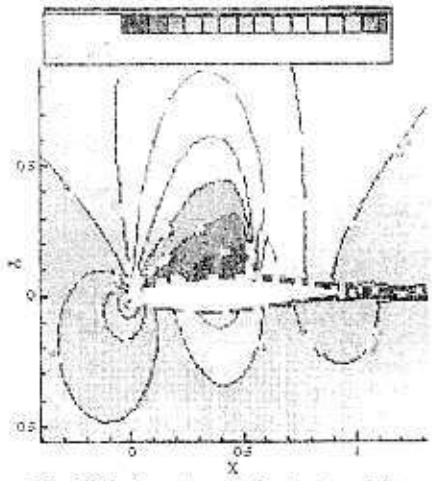

Fig 6 Mach contours (Spalart model)

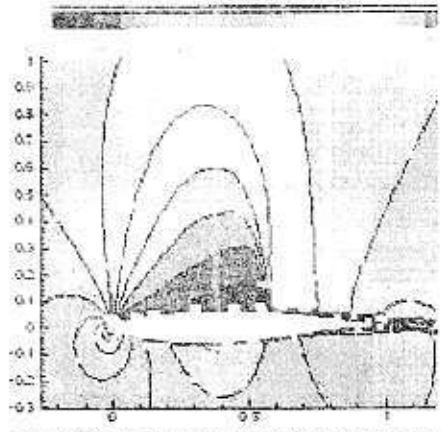

Fig 8 Mach contoud k-epsilon RNG mode

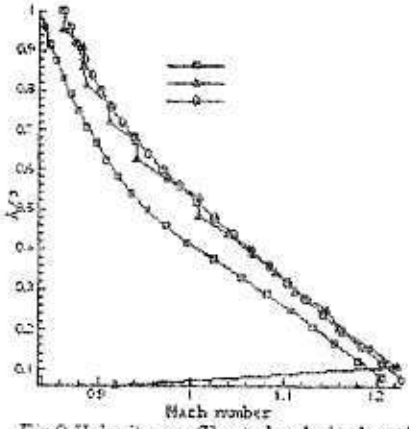

Fig.9 Velocity profile at chordwise location, x/c=0.43

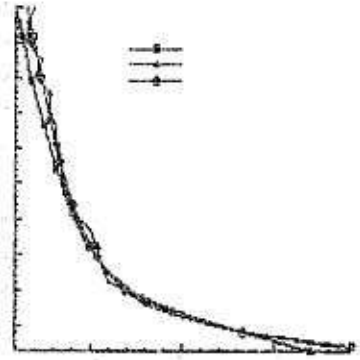

Fig.10 Velocity profile at chordwise location x/c=0.048

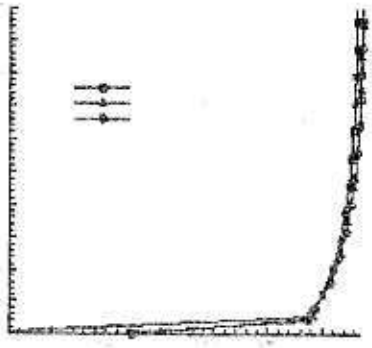

Fig.11 Velocity profile at chordwise location x/c=0.99

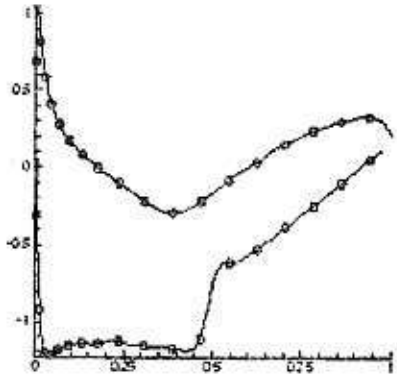

Fig.12 Pressure distribution Spalart model

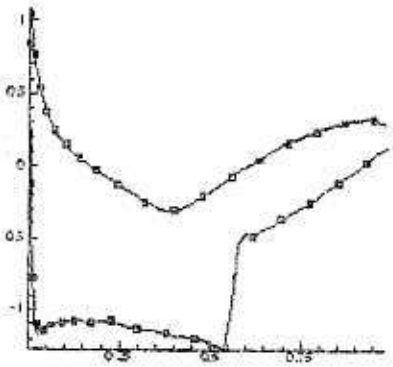

Fig.13 Pressure distribution k-epsilon standard model

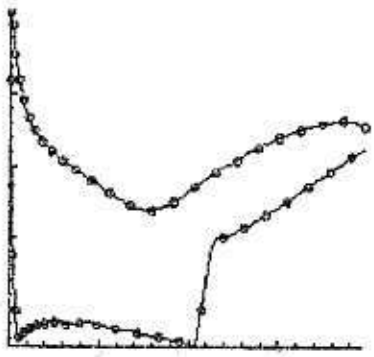

Fig.14 Pressure distribution k-epsilon RNG model

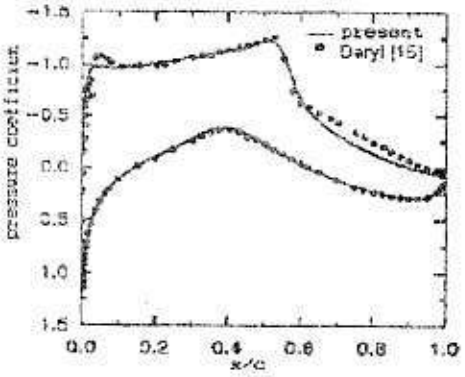

Fig.15 Pressure coefficient distribution at mach no.0.72 and alpha=2.8 deg using Spalart model

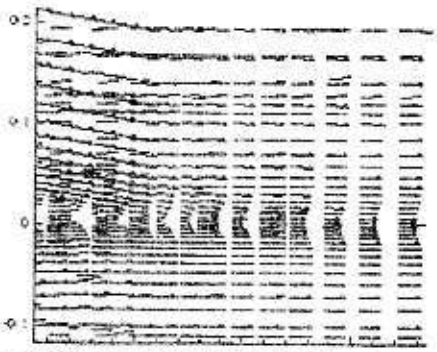

Fig.17. Velocity vectors behind trailing edge of the airfoil

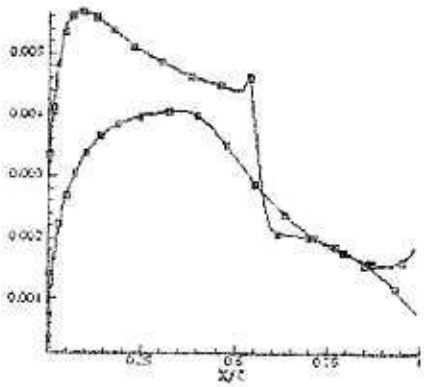

Fig.19 Skin friction coefficient profile k-epsilon standard model

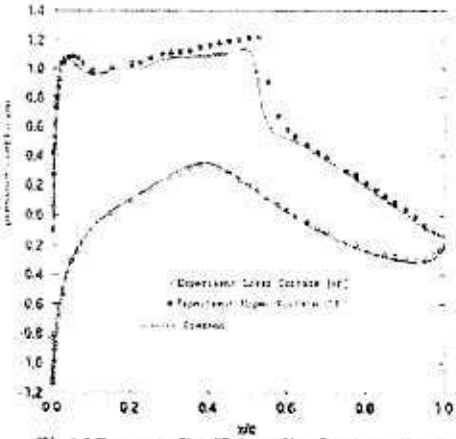

Fig.16 Pressure Coefficient distribution using k-epsilon Standard model unstructure trangular mash

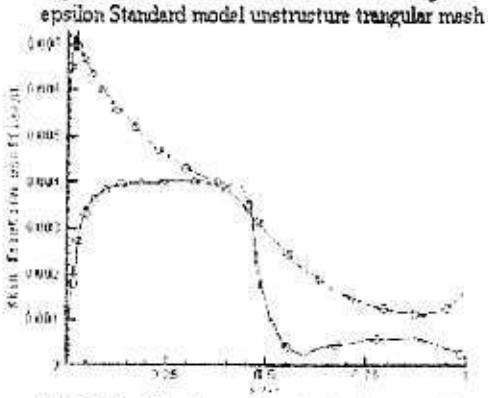

Fig.18 Skin Friction profile using Spalart model

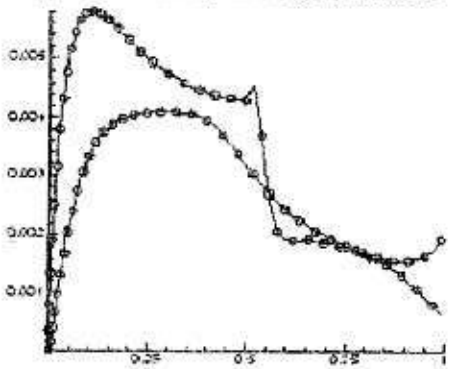

Fig.20 Skin friction profile using k-epsilon RNG

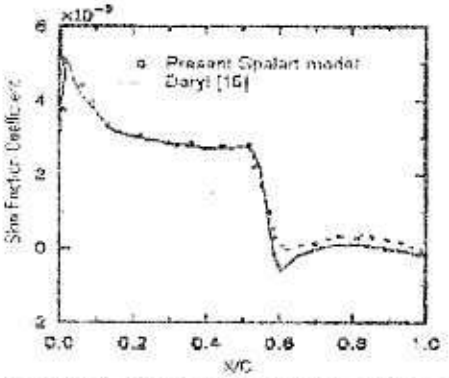

Fig.21 skin friction comparison at mach no.=0.72 and alpha 2.8 deg.

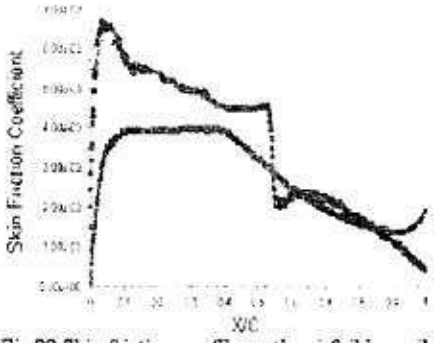

Fig.22 Skin friction profile on the airfoil k-epsilon model at mach no 0.72 and alpah 2.8 deg [14].

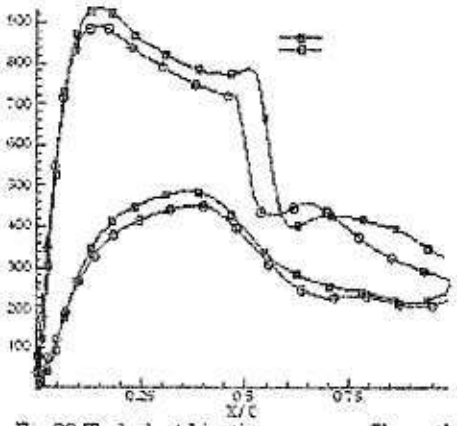

Fig.23 Turbulent kinetic energy profile on the airfoil (first grid points location)

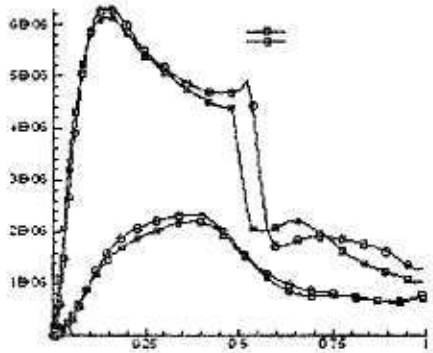

Fig.24 Dissipation energy profile on the airfoil (first grid points location)

Fig.25 Yplus distribution on the airfoil